The Journal of Immunology

RESEARCH ARTICLE | MARCH 15 2006

A Mechanism of Virulence: Virulent *Mycobacterium tuberculosis* Strain H37Rv, but Not Attenuated H37Ra, Causes Significant Mitochondrial Inner Membrane Disruption in Macrophages Leading to Necrosis [1] FREE

Minjian Chen; ... et. al

J Immunol (2006) 176 (6): 3707–3716.
https://doi.org/10.4049/jimmunol.176.6.3707

A Mechanism of Virulence: Virulent *Mycobacterium tuberculosis* Strain H37Rv, but Not Attenuated H37Ra, Causes Significant Mitochondrial Inner Membrane Disruption in Macrophages Leading to Necrosis[1]

Minjian Chen,*† Huixian Gan,* and Heinz G. Remold[2]*

Infection of human monocyte-derived macrophages with *Mycobacterium tuberculosis* at low multiplicities of infection leads 48–72 h after the infection to cell death with the characteristics of apoptosis or necrosis. Predominant induction of one or the other cell death modality depends on differences in mitochondrial membrane perturbation induced by attenuated and virulent strains. Infection of macrophages with the attenuated H37Ra or the virulent H37Rv causes mitochondrial outer membrane permeabilization characterized by cytochrome *c* release from the mitochondrial intermembrane space and apoptosis. Mitochondrial outer membrane permeabilization is transient, peaks 6 h after infection, and requires Ca^{2+} flux and B cell chronic lymphocytic leukemia/lymphoma 2-associated protein X translocation into mitochondria. In contrast, only the virulent H37Rv induces significant mitochondrial transmembrane potential ($\Delta\psi_m$) loss caused by mitochondrial permeability transition. Dissipation of $\Delta\psi_m$ also peaks at 6 h after infection, is transient, is inhibited by the classical mitochondrial permeability transition inhibitor cyclosporine A, has a requirement for mitochondrial Ca^{2+} loading, and is independent of B cell chronic lymphocytic leukemia/lymphoma translocation into the mitochondria. Transient dissipation of $\Delta\psi_m$ 6 h after infection is essential for the induction of macrophage necrosis by *Mtb*, a mechanism that allows further dissemination of the pathogen and development of the disease. *The Journal of Immunology,* 2006, 176: 3707–3716.

Tuberculosis, an infectious disease, affects 32% of the human population and causes 1.8 million deaths annually (1). Spread of tuberculosis is exacerbated due to the development of drug-resistant strains of the causative agent *Mycobacterium tuberculosis* (*Mtb*)[3] and by enhanced susceptibility of individuals infected with HIV. Importantly, only ~10% of *Mtb*-infected individuals become ill, indicating that innate immune mechanisms contain the infection in most cases (2). The predominant host cell for *Mtb* is the lung macrophages (Mϕ). Although host Mϕ are required for *Mtb* replication (3), the innate antimicrobial immune mechanisms of these cells can be activated to inhibit pathogen survival (4). Therefore, understanding the role of the Mϕ is central to understanding of innate antimycobacterial defense.

Mitochondrial damage is of key importance in the outcome of Mϕ infection with *Mtb* (5). In vitro infection of human Mϕ with attenuated *Mtb* induces predominantly apoptosis (6), a process that does not seem to be associated with the mitochondrial permeability transition (MPT)-dependent dissipation of mitochondrial transmembrane potential ($\Delta\psi_m$) (7) and contains the pathogens within apoptotic bodies (8). In contrast, infection with virulent *Mtb* causes significant necrosis following irreversible MPT and leads to spread of the infection. These findings suggest that apoptosis and necrosis should be regarded as the extremes of a continuum.

The importance of apoptosis as a critical mechanism that protects against tuberculosis has been demonstrated recently in mice. In resistant mice, the supersusceptibility to tuberculosis 1 locus (*sst1*) leads to induction of Mϕ apoptosis as a response to *Mtb* infection. In contrast, Mϕ of *sst1*-susceptible mice die after infection and show widespread necrosis (9). Thus, in vitro findings for human Mϕ and in vivo findings for mice establish apoptosis of *Mtb*-infected Mϕ as a central innate defense mechanism against tuberculosis.

In this study, we investigated the effects of attenuated and virulent *Mtb* on the integrity of the mitochondrial membranes of infected Mϕ. Low multiplicity of infection (MOI) was used as occurs in human infection. We report that inoculation of human primary Mϕ with both attenuated H37Ra and virulent H37Rv disrupts the mitochondrial outer membrane (MOM) (10–12), and that only the virulent H37Rv causes substantial loss of $\Delta\psi_m$, a consequence of MPT resulting in mitochondrial degradation and necrosis.

Materials and Methods

Materials

Thapsigargin (TG), cyclosporin A (CsA), and ruthenium red (RR) were purchased from Sigma-Aldrich; 3,3′-dihexyloxycarbocyanine iodide ($DiOC_6(3)$), rhodamine-2 AM, MitoTracker Green FM, Alexa Fluor 488, goat anti-mouse IgG1, and mouse anti-cyclooxygenase (COX) IV Ab were from

*Division of Rheumatology/Immunology, Department of Medicine, Medical Research Center Brigham and Women's Hospital, Harvard Medical School, Boston, MA 02115; and †Clinical Research Center, First Affiliated Hospital, Guangxi Medical University, Nanning, Guangxi, 530021, People's Republic of China

Received for publication August 31, 2005. Accepted for publication January 4, 2006.

The costs of publication of this article were defrayed in part by the payment of page charges. This article must therefore be hereby marked *advertisement* in accordance with 18 U.S.C. Section 1734 solely to indicate this fact.

[1] This work was supported by National Institutes of Health Grants AI50216 and HL64884.

[2] Address correspondence and reprint requests to Dr. Heinz G. Remold, Brigham and Women's Hospital, 75 Francis Street, Boston, MA 02115.

[3] Abbreviations used in this paper: *Mtb, Mycobacterium tuberculosis*; $\Delta\psi_m$, mitochondrial transmembrane potential; BAX, B cell chronic lymphocytic leukemia/lymphoma 2-associated protein X; $[Ca^{2+}]_i$, intracellular Ca^{2+} concentration; $[Ca^{2+}]_m$, intramitochondrial Ca^{2+} concentration; bid, bCL-2 homology 3 interacting death domain protein; ESAT-6, 6-kDa early secretory antigen target; CFP-10, culture filtrate protein 10; COX, cyclooxygenase; CsA, cyclosporin A; $DiOC_6(3)$, 3,3′-dihexyloxycarbocyanine iodide; Mϕ, macrophage; MOI, multiplicity of infection; MOM, mitochondrial outer membrane; MOMP, MOM permeabilization; MPT, mitochondrial permeability transition; PS, phosphatidylserine; RR, ruthenium red; siRNA, small interfering RNA; *sst1*, supersusceptibility to tuberculosis 1 locus; TG, thapsigargin.

0022-1767/06/$02.00

Molecular Probes; mouse anti-cytochrome *c* mAb (clone 7H8.2C12, 6H2.B4) and mouse IgG1 were from BD Pharmingen; rabbit anti-annexin-1 polyclonal Ab, goat anti-rabbit IgG FITC conjugate, and HRP-protein A were from Zymed Laboratories; murine anti-human actin mAb was from Pierce; rabbit anti-human B cell chronic lymphocytic leukemia/lymphoma 2-associated protein X (BAX) polyclonal Ab was from Santa Cruz Biotechnology; anti-phosphatidylserine mouse mAb (clone 1H6) and rabbit IgG were from Upstate Biotechnology; protease inhibitor mixture was from Roche; BAX small interfering RNA (siRNA) kit was from Cell Signaling Technology; and HEPES and DTT were from Invitrogen Life Technologies.

Bacteria

The *Mtb* strains H37Rv and H37Ra (American Type Culture Collection) were grown, as described before (6), and stored at −80°C. To prevent aggregates, the resuspended bacilli were sonicated for 10 s and allowed to settle for 10 min. Less than 10% of the bacteria were clumped. Before use, aliquots were sonicated twice and clumps were dispersed by 10 aspirations through a 29-gauge needle (BD Biosciences).

Quantification of mycobacteria

Adherent Mϕ were inoculated with H37Ra or H37Rv at different MOI. After 4 h, the cells were washed five times with HBSS and cultured in IMDM. To measure mycobacterial growth, cells were lysed with 500 μl of 0.2% SDS in PBS. SDS was neutralized by addition of 500 μl of 50% FCS. A total of 100 μl of cell lysates from triplicate cultures was serially diluted 10-fold and plated on 7H10 agar plates (REMEL), and colonies were counted after 21 days. Alternatively, the cell lysates were pooled and inoculated into triplicate Bactec 12B vials. The number of mycobacterial was determined by use of the Bactec model 460TB system (BD Biosciences).

Cells and culture

Mononuclear cells from peripheral blood of healthy donors under informed consent and harvested under guidelines approved by the Brigham and Women's Hospital Human Studies Committee were isolated, as previously described (5). Mϕ were cultured for 7 days in IMDM (Invitrogen Life Technologies) containing 10% human AB serum (Gemini Bio-Products) and challenged with varying MOI of *Mtb*, as described.

In situ analysis of programmed cell death

Apoptosis of Mϕ infected with virulent and attenuated *Mtb* was determined by use of a fluorescent in situ TUNEL assay (In Situ Cell Death Detection Kit; tetramethylrhodamine red; Roche) according to the manufacturer's specifications. Necrosis was determined by counting the number of adherent cells at varying times after infection using an inverted phase contrast microscope (Nikon) equipped with a 10-mm^2 grid in the eyepiece. Three wells per condition were counted at a magnification of ×100. All plates were assigned coded identification by an individual not involved in the study.

Necrosis of Mϕ infected with virulent and attenuated *Mtb* was assessed using light microscopy of fixed and May-Grünwald-Giemsa-stained samples.

Flow cytometric analysis of mitochondrial cytochrome c *release in Mϕ (Mϕ surface phosphatidylserine (PS) and annexin-1)*

After diffusion of cytochrome *c* from the cytoplasm, Mϕ with intact mitochondria stain positive for cytochrome *c*, while cells with mitochondria unable to retain mitochondrial cytochrome *c* stain negative (13). Mϕ were cultured at 1.5×10^6 cells/2 ml/well in 6-well cluster plates (Corning Glass), washed with ice-cold PBS, and treated with 50 μg/ml digitonin in ice-cold PBS containing protease inhibitor mixture for 5 min on ice to allow selective permeabilization of the plasma membrane. After three washes with PBS, Mϕ were fixed with 1% paraformaldehyde for 20 min at room temperature, dislodged from plates with a rubber policeman, pelleted at 500 × *g*, washed, and incubated in PBS containing 3% BSA and 0.05% saponin for 1 h. The cells were then incubated with mouse anti-cytochrome *c* mAb clone 6H2.B4 (BD Biosciences; 1/200 dilution) overnight at 4°C and with Alexa Fluor 488 goat anti-mouse IgG1 (1/200 dilution) for 1 h at room temperature, washed, resuspended in PBS containing 1% BSA, and analyzed under FL-1 logarithmic amplification by FACS. Mϕ stained with irrelevant isotype Ab were used as controls.

For flow cytometric analysis of Mϕ surface PS and annexin-1 (14, 15), Mϕ were washed twice with ice-cold PBS containing 1% BSA after infection for 6 h, and incubated for 30 min on ice with mouse anti-PS monoclonal IgG (Upstate Biotechnology) or rabbit anti-annexin-1 polyclonal Ab (Zymed Laboratories) at a dilution of 1/200 in FACS buffer. After washing with ice-cold PBS containing 1% BSA, cells were incubated for 20 min with goat anti-mouse Alexa Fluor 488 (Molecular Probes) for PS-FACS analysis, or goat anti-rabbit FITC conjugate (Zymed Laboratories) for annexin-1-FACS analysis. Cells were then fixed with 1% paraformaldehyde for 20 min. Green fluorescence was measured by FACS analysis. Mϕ stained with irrelevant isotype Ab were used as controls.

Assessment of cytochrome c *release from the mitochondria by Western blotting*

Mϕ were cultured at a density of 1.5×10^6 mononuclear cells/2 ml/well in 6-well cluster plates (Corning Glass) (5). The cells were infected with H37Rv at an MOI of 10:1 for 6, 12, and 48 h, washed with ice-cold PBS, and treated with 50 μg/ml digitonin in PBS in the presence of protease inhibitor mixture (Roche) for 5 min on ice. The digitonin solution was replaced with 500 μl of ice-cold extract buffer (250 mM sucrose, 20 mM HEPES (pH 7.5), 50 mM KCl, 2.5 mM $MgCl_2$, 1 mM DTT, and protease inhibitor mixture). The cells were incubated for 20 min on ice, dislodged with a rubber policeman, and centrifuged at 1000 × *g*. A total of 20 μg of the supernatant protein was resolved in 15% SDS-PAGE gel. The polypeptides were transferred to polyvinylidene difluoride transfer membrane (PerkinElmer), treated with blocking buffer (5% nonfat dry milk in TBST), and incubated with mouse anti-cytochrome *c* mAb (clone 7H8.2C12, 1/500 dilution in blocking buffer). Actin was used as loading control. After extensive washing with TBST, membranes were incubated with HRP-protein A at room temperature for 1 h, and the polypeptides were developed with Western Lighting Chemiluminescence (PerkinElmer Life Sciences) by exposure to x-ray films.

Assessment of MPT in Mϕ

MPT was assessed in Mϕ by evaluation of mitochondrial membrane potential (Δ_m) dissipation by measuring retention of the lipophilic cationic dye $DiOC_6(3)$ within the mitochondria (16). Cells were preloaded with 1.5 nM $DiOC_6(3)$ in IMDM for 20 min at 37°C, washed, and incubated at 37°C for 10 min in medium containing 15 μg/ml digitonin, washed, and fixed with 1% paraformaldehyde for 20 min at 25°C. Cells were dislodged with a rubber policeman, pelleted at 500 × *g*, washed, and resuspended in PBS containing 1% paraformaldehyde. Flow cytometry to detect cells with diminished fluorescence was performed under FL-1 logarithmic amplification using FACS. Mϕ stained with irrelevant isotype Ab were used as controls. In preliminary experiments, we tested whether fixation with paraformaldehyde alters the staining with the cationic dye $DiOC_6(3)$. After preloading with the dye, cells were fixed with 1% paraformaldehyde or not fixed before FACS analysis. No significant difference in $DiOC_6(3)$ fluorescence was detected.

Transfection of Mϕ with BAX siRNA

Mϕ were transfected with BAX siRNA using a BAX siRNA kit (Cell Signaling Technology), following the protocol of the manufacturer. Mϕ plated at 1×10^6 cells/ml/well in 6-well cluster plates (Corning Glass) were cultured in IMDM with 10% human AB serum. Fresh medium was added to the cells 1 day before transfection. BAX siRNA or nontargeted siRNA (100 nM) were added to the cells. To determine RNA silencing of BAX expression, Mϕ were transfected for 72 h, and the cells were then lysed in 1× SDS sample buffer. Cell lysates were fractionated on 15% SDS-PAGE using p42 as a loading control. To measure BAX translocation into mitochondria, infected Mϕ were dislodged and resuspended in PBS containing 500 μg/ml digitonin and protease inhibitor mixture for 5 min and centrifuged at 16 000 × *g* for 20 min. After washing, the pellets were dissolved in 1× sample buffer, and 20 μg was resolved on 15% SDS-PAGE using COX IV as a loading control. To measure cytochrome *c* and $DiOC_6(3)$ release in siRNA-transfected Mϕ after *Mtb* infection by FACS, the cells were transfected for 72 h, as described. The transfected cells in IMDM containing 2% human AB serum were inoculated with *Mtb* and were then prepared, as described for FACS analysis.

Confocal fluorescence imaging of intramitochondrial Ca^{2+} in Mϕ

Mϕ were cultured in 35-mm glass-bottom microwell dishes at 1.5×10^6 mononuclear cells/2 ml/well, infected with 10 H37Ra/cell for varying times, and then washed with IMDM. Cells were then preloaded with 2 μM dihydrorhodamine-2 AM (prepared by reduction of rhodamine-2 AM following the manufacturer's protocol) for 30 min at 4°C in IMDM containing 10% AB serum, incubated for 2 h at 37°C in IMDM without serum, and then loaded with 50 nM MitoTracker Green FM in IMDM without serum at 37°C for 15 min. The cells were washed twice and resuspended in 500 μl of medium, and confocal images of rhodamine-2 and MitoTracker Green were acquired with a Nikon TE-2000U laser-scanning confocal microscope using excitation wave lengths of 488 and 543 nm and emission wavelengths of 516 and 570 nm for MitoTracker Green and rhodamine-2,

respectively. All images were acquired at 37°C using a temperature-controlled chamber. Mitochondria were identified by the green fluorescence of the MitoTracker Green.

Histology

Mϕ (2.5×10^5/ml/well) were cultured on 12-mm-diameter coverslips (Propper Manufacturing) for 7 days to allow attachment. After infection with *Mtb* for 48 h, the cells were washed twice with IMDM and fixed in methanol:acetic acid (3:1 vol) for 24 h. The cells were stained with Wright's stain (Fisher Scientific) for 10 min and Giemsa stain for 20 min. The cells were then examined by light microscopy and were photographed with a Leica DFC300 digital camera.

Electron microscopy

Mϕ were cultured in IMDM containing 10% human AB serum in a 6-well plate. The cells were infected with H37Rv or H37Ra (MOI 10) for 48 h, fixed with 100 mM cacodylate buffer (1.25% formaldehyde, 2.5% glutaraldehyde, and 0.03% picric acid) overnight at 4°C, and postfixed in 1% osmium tetroxide containing 1.5% potassium ferrocyanide for 30 min. The cells were then stained with 1% uranyl acetate in maleate buffer (pH 5.2) for 30 min at room temperature. After dehydration, the cells were removed from the plate in propylene oxide and centrifuged at $3000 \times g$ for 3 min. Pellets were incubated in a 1:1 mixture of propylene oxide and Epon (TAAB Epon; Marivac) for 2 h at room temperature, embedded with TAAB Epon, and polymerized for 48 h at 60°C. Sections (80 nm) were mounted on copper grids, stained with 2% uranyl acetate in acetone, followed by 0.2% lead citrate, examined in a JEOL 1200EX transmission electron microscope (JEOL), and recorded on Kodak sheet film (Eastman Kodak).

Statistics

Results are expressed as mean ± SE. The data were analyzed by using Microsoft Excel Statistical Software (Jandel) using *t* test for normally distributed data with equal variances. A p value <0.05 was considered statistically significant.

Results

Virulent H37Rv and attenuated H37Ra induce transient release of cytochrome c *from the mitochondria in Mϕ*

In the mitochondrial pathway of apoptosis, MOM permeabilization (MOMP) leads to release of proapoptotic factors, including apoptosis-inducing factor, Htr2/Omi, endo 6, Smac/Diablo, and cytochrome *c* from the mitochondrial intermembrane space into the cytosol, resulting in the activation of downstream caspases and apoptosis (see online supplement to Ref. 7). To assess the effect of virulent and attenuated *Mtb* on Mϕ MOMP, Mϕ were inoculated with H37Ra or H37Rv, and cytochrome *c* release was measured by flow cytometry as a function of time. The number of cells with depleted mitochondrial cytochrome *c* is up-regulated at 6 h after infection (Fig. 1, *A* and *B*). At 12 and 24 h, the number of cytochrome *c*-depleted Mϕ has almost returned to baseline levels, indicating that MOM impermeability recovers. At 48 h, the number of cells with depleted mitochondrial cytochrome *c* increases again (Fig. 1, *A* and *B*), reflecting $\Delta\psi_m$ dissipation associated with mitochondrial degradation and necrotic death (10).

In dose-response experiments, H37Ra and H37Rv at MOI of ≤ 2 minimally increase mitochondrial cytochrome *c* release at 6 h (Fig. 1*C*). At MOI 5, H37Rv produces more Mϕ with depleted mitochondrial cytochrome *c* than H37Ra ($p = 0.01$), and at MOI 10 both strains generate comparable numbers of Mϕ with depleted mitochondrial cytochrome *c*.

These results could be confirmed by Western blotting of cytochrome *c* translocated into the cytosol of H37Rv-infected Mϕ. The cytochrome *c* concentration in the cytosol is increased at 6 and

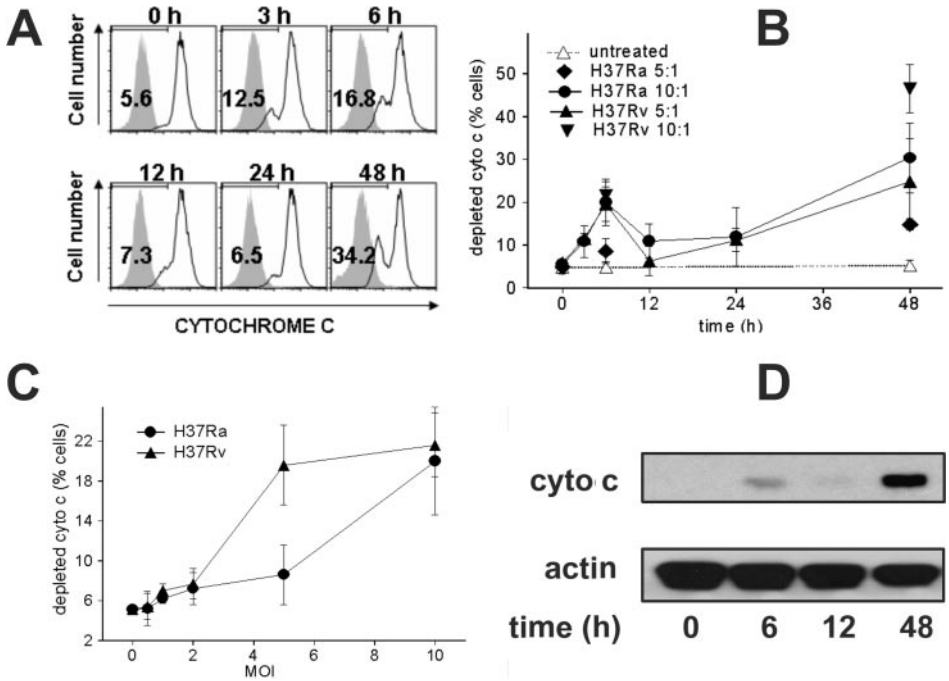

FIGURE 1. Release of mitochondrial cytochrome *c* in Mϕ infected with attenuated *Mtb* strain H37Ra and virulent strain H37Rv. Mϕ were inoculated with the indicated MOI, cultured for the indicated times (*A*, *B*, or for 6 h (*C*)), harvested, permeabilized, stained with cytochrome *c* Ab, and analyzed by FACS. *A*, Histograms show a representative experiment for Mϕ infected with H37Ra at MOI 10 after staining with cytochrome *c* Ab (open profiles). The shaded profiles indicate Mϕ stained with irrelevant isotype Ab. The gate to select Mϕ with depleted cytochrome *c* is indicated by the bar on the *top*. *B*, Summary of three experiments for H37Ra (●, ♦) and H37Rv (▲, ▼) at the indicated MOI. Mϕ infected with H37Ra at MOI 5 (♦) and with H37Rv at MOI 10 (▼) were examined only at 6 and 48 h. The difference between the numbers of Mϕ with depleted mitochondrial cytochrome *c* at 0 time and 6 h was statistically significant for H37Rv ($p = 0.01$) and H37Ra/MOI 10 ($p = 0.02$). Cytochrome *c* release at 6 h reflects MOMP; loss at 48 h reflects the mitochondrial degradation that precedes Mϕ necrosis (detailed below). *C*, Dose response. Shown are mean values ± SE for four experiments for Mϕ infected with H37Ra and H37Rv at the indicated MOI, harvested, and analyzed at 6 h. *D*, Mitochondrial cytochrome *c* translocation into the cytosol of Mϕ infected with H37Rv (MOI 10) as determined by Western blotting is seen 6 and 48 h after infection. No extramitochondrial cytochrome *c* accumulation is detected 12 h after infection.

48 h after inoculation with H37Ra. No cytochrome *c* accumulation is detectable 12 h after inoculation (Fig. 1*D*).

We further tested whether MOMP is associated with an increase of the apoptotic markers PS and annexin-1 (14, 15, 17). Infection of Mϕ with H37Ra increases the number of Mϕ with augmented PS on the cell surface. The increase of Mϕ with augmented cell surface PS is not statistically different from untreated controls, when Mϕ are infected with H37Rv, indicating that induction of apoptotic markers by the virulent H37Rv is attenuated when compared with infection with H37Ra (6). In contrast, infection of Mϕ with H37Ra and with H37Rv increased levels of cell surface annexin-1 at 6 and 24 h after infection (Fig. 2). The increase of the numbers of Mϕ with augmented surface annexin-1 is significantly smaller, when the cells are infected with H37Rv.

Virulent H37Rv, but not attenuated H37Ra, induces significant dissipation of $\Delta\psi_m$

We next investigated whether *Mtb* induces opening of the inner mitochondrial membrane. MPT pore opening associated with mitochondrial inner membrane perturbation is an independent event that frequently accompanies MOMP (7). When the permeability transition pore opens, collapse of the mitochondrial inner membrane potential $\Delta\psi_m$ ensues as a consequence of dissipation of the proton gradient generated in the mitochondrial intermembrane space. Opening of the permeability transition pore uncouples the respiratory chain and causes overproduction of superoxide anions (16, 18), leading to necrosis. To test whether virulent and attenuated *Mtb* strains differ in their capacity to induce $\Delta\psi_m$ dissipation, we infected Mϕ with H37Ra and H37Rv. H37Ra was initially used at MOI 10 and H37Rv at MOI 5 to equalize cytochrome *c* release at 6 h. Transient MPT determined by FACS quantification of cells with depleted $DiOC_6(3)$ is maximal for both *Mtb* strains at 6 h after infection (Fig. 3, *A* and *B*) and is significantly greater, when Mϕ are infected with H37Rv than with H37Ra ($p = 0.01$) (Fig. 3*B*). At 12 and 24 h, the number of Mϕ with depleted mitochondrial $DiOC_6(3)$ has returned almost to baseline in both cultures, indicating that MPT at 6 h is transient and mitochondrial inner membrane impermeability has recovered. Dose-response studies indicate that H37Rv is ~4 times more effective as an inducer of MPT than H37Ra (Fig. 3*C*). At 36 and 48 h, H37Rv induces greater numbers of Mϕ with depleted mitochondrial $DiOC_6(3)$, a correlate of the prenecrotic state of the cells, than H37Ra ($p = 0.009$ at 36 h; $p = 0.018$ at 48 h). We next compared the dose response of H37Rv with respect to MPT and MOMP at 6 h. At low MOI (0.5 and 2), H37Rv induces significant MPT while leaving MOM intact (Fig. 3*D*). The difference of the number of Mϕ with depleted mitochondrial cytochrome *c* or depleted mitochondrial $DiOC_6(3)$ at 6 h is statistically significant at MOI 0.5 ($p = 0.01$) and MOI 2 ($p = 0.001$; Fig. 3*D*) and indicates that MPT at 6 h occurs in Mϕ with intact MOM, and that these cells might proceed directly to undergo necrosis. MPT without MOMP was also reported in granzyme A-treated apoptotic K562 cells (19).

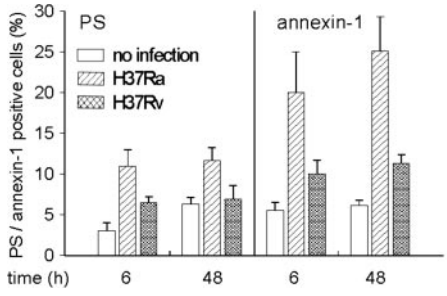

FIGURE 2. Exposure of the apoptotic markers PS and annexin-1 on the Mϕ surface is up-regulated after *Mtb* inoculation. Mϕ were inoculated with H37Ra and H37Rv (MOI 10), harvested after 6 and at 48 h, stained for PS or for annexin-1, and examined by FACS. The difference in the increase of the numbers of Mϕ with augmented surface PS in comparison with noninfected Mϕ cultures is statistically significant for both time points in H37Ra-infected Mϕ cultures ($p < 0.02$, $n = 3$), but not in H37Rv-infected Mϕ cultures ($p > 0.12$, $n = 3$). The difference in increase of Mϕ numbers with augmented cell surface annexin-1 in comparison with noninfected cultures is statistically significant for both time points for H37Ra ($p < 0.05$, $n = 3$)- and H37Rv ($p < 0.04$, $n = 3$)-infected Mϕ.

We further tested whether differential uptake of H37Ra and H37Rv by the Mϕ accounts for differential induction of MPT and MOMP. To that end, we measured phagocytosis of H37Ra and H37Rv after 4 h of incubation of the Mϕ with both strains at various MOI. The number of ingested bacteria was not found to be different for H37Ra and H37Rv (Fig. 3*E*).

Consistent with these results, Mϕ infected with H37Rv undergo more necrosis than cultures infected with H37Ra, because more Mϕ are undergoing cytolysis in H37Rv-infected Mϕ cultures than in cultures infected with H37Ra. As assessed by light microscopy 72 h after infection with H37Ra (MOI 10), the percentage of Mϕ undergoing cytolysis was 36 + 14%. In contrast, Mϕ cultures infected with H37Rv (MOI 10) contained at 72 h 82 + 5% Mϕ undergoing cytolysis. Pretreatment of the H37Rv-infected Mϕ cultures with CsA (5 μM) reduced the number of necrotic cells to 29 + 13%. The difference between these values is statistically significant ($p < 0.005$, $n = 3$).

With respect to this study, the important difference between apoptosis and necrosis is the lack of Mϕ plasma membrane integrity associated with necrosis. In contrast, apoptotic Mϕ have intact plasma membranes that prevent exocytosis of inflammatory components from the cytoplasm and allow containment of the pathogens within the cells. Mϕ infected for 48 h with H37Ra (MOI 10) show signs of apoptosis such as pycnotic nuclei, but have intact plasma membranes. In contrast, Mϕ infected with the virulent H37Rv show significant disruption of the plasma membrane (Fig. 4).

Because in some cells cell death induced by MOMP is abrogated by caspase inhibitors (20), we tested whether $\Delta\psi_m$ loss of H37Rv-infected Mϕ is dependent on caspase activation. To that end, we treated Mϕ with the pan-caspase inhibitor zVAD-fmk before inoculation. Caspase inhibition does not decrease $\Delta\psi_m$ loss in these cells. The number of Mϕ with cationic dye release in absence of zVAD-fmk was 45.8 ± 3.5% and in presence of the inhibitor 44.6 ± 3.8% ($p > 0.1$, $n = 3$), indicating that induction of MOMP by *Mtb* is caspase independent.

Ca^{2+} flux into the mitochondria is required for MOMP and MPT of Mtb*-infected Mϕ*

In many cell systems, increase of mitochondrial Ca^{2+} levels is required for MOMP (21) and is also an important modulator of MPT (22). We therefore investigated whether after infection with *Mtb* mitochondrial Ca^{2+} loading is important for the induction of MOMP and MPT. Mϕ were preincubated with RR, an inhibitor of the mitochondrial Ca^{2+} uniporter (23) that prevents mitochondrial calcium loading, and were inoculated with H37Ra and H37Rv, and MOMP and MPT were measured (Fig. 5*A*). Pretreatment with RR inhibits both mitochondrial cytochrome *c* release and release of $DIOC_6(3)$ of H37Ra and H37Rv-inoculated Mϕ, indicating that mitochondrial Ca^{2+} loading is required for the induction of MOMP and of MPT. Addition of RR to uninfected cells has no effect. Furthermore, pretreatment of Mϕ with TG, a sarcoplasmic/endoplasmic reticulum calcium ATPases pump inhibitor that causes passive Ca^{2+} release from the endoplasmatic reticulum

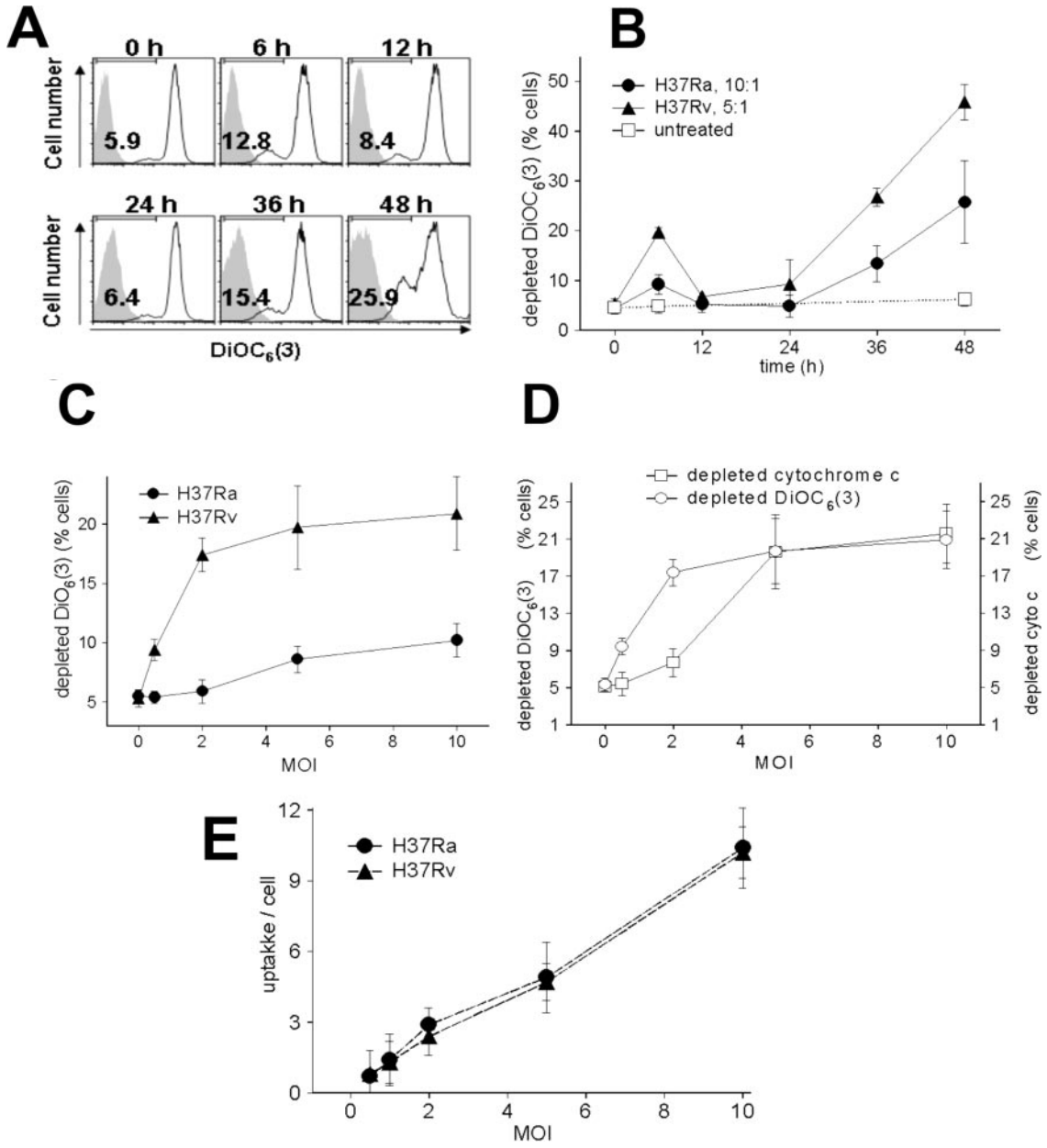

FIGURE 3. Induction of MPT in Mϕ infected with attenuated H37Ra and virulent H37Rv. MPT was assayed by quantifying cells with depletion of the mitochondrial cationic dye $DiOC_6(3)$. *A* and *B*, Time course. *A*, The histograms show a representative experiment in which Mϕ were infected with H37Ra (MOI 10). The shaded profiles indicate Mϕ unstained. The gate to select Mϕ with depleted cationic dye is indicated by bars at the *top*. *B*, Summary of three experiments for H37Ra (MOI 10) and H37Rv (MOI 5). Shown are mean values $\pm$ SE. *C*, Dose response. Shown are mean values $\pm$ SE for H37Ra and H37Rv. Mϕ infected at the indicated MOI were assayed after 6 h. The difference in the numbers of Mϕ with diminished mitochondrial cationic dye is statistically significant for two *Mtb* strains at MOI 2, 5, and 10 ($p < 0.026$). *D*, Dose response of the effect of different MOI of H37Rv on MPT (○) and MOMP (□) at 6 h after infection. Note that H37Rv at MOI 0.5 and 2 induces significant MPT while leaving MOM intact. *E*, Uptake of H37Ra and H37Rv by Mϕ after 4-h incubation (MOI indicated on the abscissa) is identical over a wide range of MOI ($p > 0.3$).

stores and concomitant increases of intramitochondrial Ca^{2+} concentration ($[Ca^{2+}]_m$) (24), augments MPT and MOMP. Treatment with TG to increase mitochondrial calcium loading augments exposure of the apoptotic markers PS and annexin-1 on the Mϕ surface, and RR treatment to decrease mitochondrial Ca^{2+} levels substantially diminishes surface expression of both apoptotic markers (data not shown).

To demonstrate that infection with *Mtb* indeed leads to Ca^{2+} influx into the mitochondria, we analyzed H37Ra-infected Mϕ by confocal fluorescence microscopy using rhodamine-2, a Ca^{2+}-sensitive fluorescent dye that preferentially accumulates in mitochondria (25) and MitoTracker Green to label the mitochondria (26). This approach revealed an increase of $[Ca^{2+}]_m$ at 6 h coincident with the peak of transient MOMP and $\Delta\psi_m$ loss (Fig. 5*B*, *row 2*) that is not found at 12 or 24 h (Fig. 5*B*). More than 90% of the Mϕ contained increased $[Ca^{2+}]_m$ at 6 h (data not shown). TG (0.2 μM) further increased $[Ca^{2+}]_m$ in H37Ra-infected Mϕ at 6 h, and RR abrogated the Ca^{2+} uptake into mitochondria induced by H37Ra.

Translocation of BAX to the mitochondria is required for MOMP; $\Delta\psi_m$ dissipation is independent of BAX translocation

Apoptosis is initiated by cleavage and activation of cytosolic BID by proteases that cause translocation of BAX into the mitochondria and activation of BAK, resulting in the release of cytochrome *c*

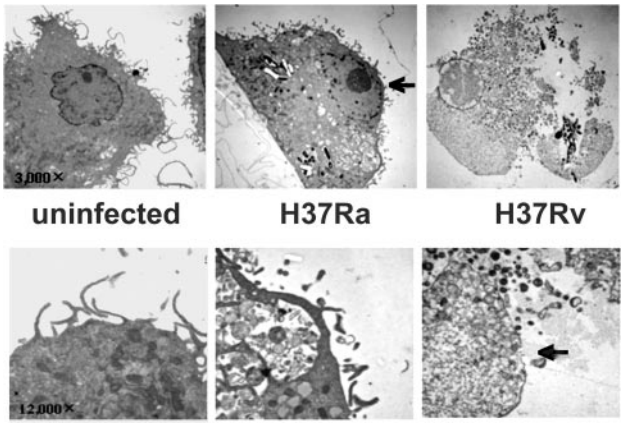

FIGURE 4. Morphology of Mϕ infected with the attenuated H37Ra and the virulent H37Rv. Mϕ infected with H37Ra and H37Rv for 48 h were processed for electron microscopical examination (see *Materials and Methods*). *Upper panels*, Pictures of single cells at a magnification of ×3,000; *lower panels*, sections of the plasma membrane of the same cell at a magnification of ×12,000. Note that H37Ra induces apoptosis characterized by nuclear pycnosis (*upper center panel*, arrow) and intactness of the plasma membrane (*center panels*). In contrast, H37Rv causes destruction of the plasma membrane (*right panels*). The arrow in the *lower right panel* indicates where the continuity of the plasma membrane is interrupted. An uninfected Mϕ is seen in the panels on the *left*.

into the cytosol and in apoptosis (27, 28). To test the role of BAX in *Mtb*-induced Mϕ death, we examined the translocation of the cytoplasmic protein BAX into the mitochondria of infected Mϕ. BAX was found to be associated with mitochondria at 3 h and at all later time points after inoculation with H37Ra or with H37Rv (Fig. 6*A*). BAX redistribution was not affected by changes in Ca^{2+} flux into the mitochondria (Fig. 6*B*). RR (23), an inhibitor, and TG, a promoter of Ca^{2+} flux into the mitochondria (24), do not alter BAX translocation.

Treatment of infected Mϕ with BAX siRNA decreases BAX expression (Fig. 6*C*) and blocks mitochondrial cytochrome *c* release at 6 h (Fig. 6*D*), demonstrating that BAX translocation is required for MOMP. In contrast, abrogation of BAX expression does not inhibit mitochondrial $DiOC_6(3)$ depletion. MPT proceeds irrespective whether BAX is translocated into the mitochondria or not (Fig. 6*E*). This is not surprising, because BAX activation is a prerequisite for MOMP (28) and independent of MPT.

MOMP and MPT are associated with apoptosis and necrosis, respectively

We next performed experiments to investigate whether MOMP is associated with the induction of apoptosis. Infection of Mϕ with H37Ra (MOI 10) induces MOMP 6 h after infection, and MPT induction is negligible (Fig. 3*B*). Up-regulation of cell surface exposure of the apoptotic markers PS and annexin-1 also indicates that MOMP and not MPT is associated with apoptosis (Fig. 2). At 48 h, the number of TUNEL-positive Mϕ is also significantly increased under these infection conditions (Fig. 7*A*, *left panel*).

Treatment of Mϕ with CsA (5 μM), a classic inhibitor of MPT, does not inhibit accumulation of TUNEL-positive Mϕ (Fig. 7*A*, *left panel*), accumulation of Mϕ with depleted mitochondrial cytochrome *c* at 6 h (Fig. 7*B*), and of Mϕ with increased surface exposure of PS and annexin-1 (Fig. 7*C*). These findings indicate that MPT is independent of MOMP (7). In contrast, susceptibility of necrosis (Fig. 7*A*, *right panel*) and of mitochondrial $DiOC_6(3)$ depletion, an indicator of $\Delta\psi_m$ loss (Fig. 7*D*), to the effect of CsA shows that these events are caused by MPT (16).

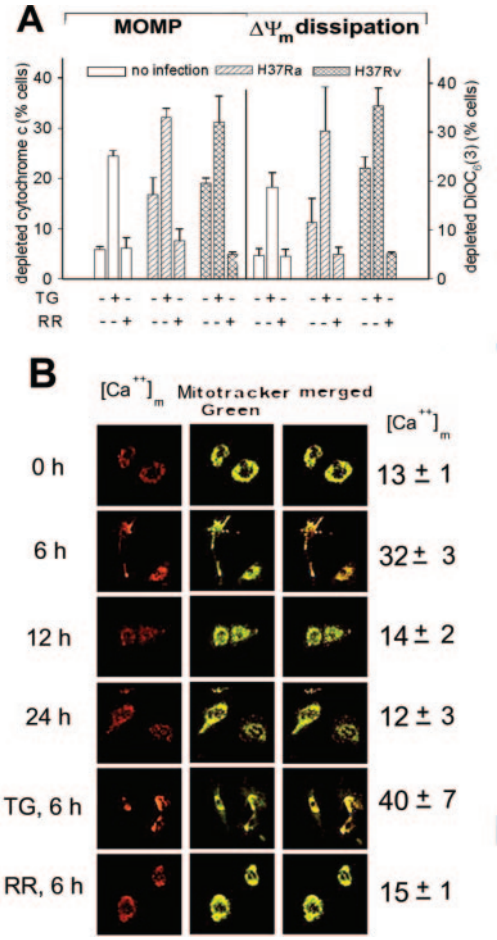

FIGURE 5. Changes in $[Ca^{2+}]_m$ in Mϕ following *Mtb* infection alter MOMP and $\Delta\psi_m$ loss induced by *Mtb*. *A*, Mϕ treated either with 0.2 μM TG that up-regulates $[Ca^{2+}]_m$ or with 5 μg/ml RR that blocks Ca^{2+} uptake into the mitochondria were infected with the attenuated H37Ra (MOI 10) or with the virulent H37Rv (MOI 10) for 6 h. The cells were harvested, and cytochrome *c* (MOMP) and $DiOC_6(3)$ release from the mitochondria reflecting $\Delta\psi_m$ loss were measured. Shown are mean values ± SE for three experiments. TG enhances cytochrome *c* ($p < 0.009$, $n = 3$) and $\Delta\psi_m$ loss (cationic dye release) ($p < 0.03$, $n = 3$) induced by H37Ra and H37Rv. RR blocks cytochrome *c* and $\Delta\psi_m$ loss ($p < 0.02$, $n = 3$). *B*, Uninfected Mϕ (0 h) or H37Ra-infected Mϕ (MOI 10) were harvested at the indicated times and stained with MitoTracker Green for mitochondria and rhodamine-2 (red) for intramitochondrial $[Ca^{2+}]_m$ and examined by confocal microscopy. A representative experiment of five experiments is shown. The mean values ± SE ($n = 3$) on the *right side* of the panel represent quantification of $[Ca^{2+}]_m$ (rhodamine-2 fluorescence) using Adobe Photoshop. $[Ca^{2+}]_m$ increases transiently at 6 h after *Mtb* inoculation and is further increased by 0.2 μM TG. In the presence of RR (5 μg/ml), $[Ca^{2+}]_m$ failed to increase at 6 h after infection. The difference between control and 6-h infection and control and 6-h infection in presence of TG was statistically significant ($p < 0.0001$, $n = 20$).

When multiple *Mtb* infection studies are subjected to linear regression analysis, the extent of transient $\Delta\psi_m$ loss at 6 h correlates with the number of Mϕ entering the necrotic state at 48 h (Fig. 8*A*), suggesting that up-regulation of early MPT commits the Mϕ to necrosis at 48 h.

Up-regulation of the numbers of Mϕ with depleted cytochrome *c* in comparison with the number of cells with cationic dye depletion at 6 h correlates with diminished numbers of prenecrotic cells at 48 h (Fig. 8*B*). These findings indicate a possible protective effect of MOMP. Alternatively, attenuated *Mtb* might induce

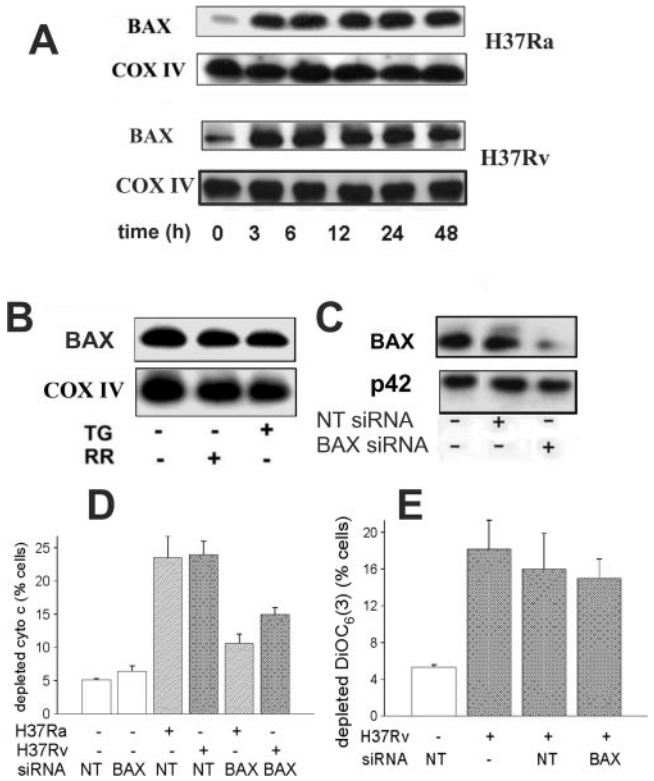

FIGURE 6. BAX translocation into mitochondria of *Mtb*-infected Mϕ and effect of silencing of BAX. *A*, Time course of BAX translocation. Mϕ infected with H37Ra and H37Rv (MOI 10) were harvested at the indicated times, and BAX content of mitochondria was measured by Western blot with COX IV as loading control. One experiment representative of three is shown. *B*, Lack of effect of TG (0.2 μM) and RR (5 μg/ml) on BAX translocation. Mϕ were harvested 6 h postinfection, and mitochondria were examined. *C–E*, Effect of BAX siRNA silencing. Mϕ were pretreated for 72 h by mock transfection, transfection with nontargeted (NT) or BAX siRNA, infected with H37Ra (MOI 10), and harvested 6 h later. *C*, Cell lysates were analyzed for content of BAX, with p42 MAPK (p42) used as loading control. One experiment representative of four is shown. *D*, Cytochrome *c* release from mitochondria. Shown are mean values ± SE for three experiments. Note that BAX silencing blocks early release of mitochondrial cytochrome *c* of infected Mϕ ($p = 0.001$). *E*, $DiOC_6(3)$ release from mitochondria reflecting MPT. Shown are mean values ± SE for three experiments. Note that BAX silencing by targeted siRNA (data not shown) does not affect mitochondrial $DiOC_6(3)$ depletion ($p = 0.3$).

changes in the mitochondria that cause MPT accompanied by MOMP, favoring apoptosis, and virulent *Mtb* might increase MPT, but inhibit MOMP, leading to increased necrosis.

Discussion

The major findings of this study are that the virulent H37Rv induces significantly more MPT and $\Delta\psi_m$ dissipation than the attenuated H37Ra 6 h after infection of the Mϕ. In contrast, both the attenuated *Mtb* strain H37Ra and the virulent strain H37Rv cause MOMP. Both MPT and MOMP at 6 h are transient, and the capacity of MOM to retain cytochrome *c* has largely recovered at 12 and 24 h after infection. Reversible MOMP is also induced in isolated THP-1 mitochondria, when incubated with cytosol from Mϕ infected for 6 h, suggesting a role for cytosolic factors and not a direct effect of *Mtb* on the mitochondria in the induction of MOMP (data not shown). Induction of MOMP is associated with the appearance of the early apoptotic markers PS and annexin-1 on the Mϕ surface. In contrast to MOMP, H37Rv-induced MPT at 6 h is blocked by CsA, a classic inhibitor of MPT. Using agents that

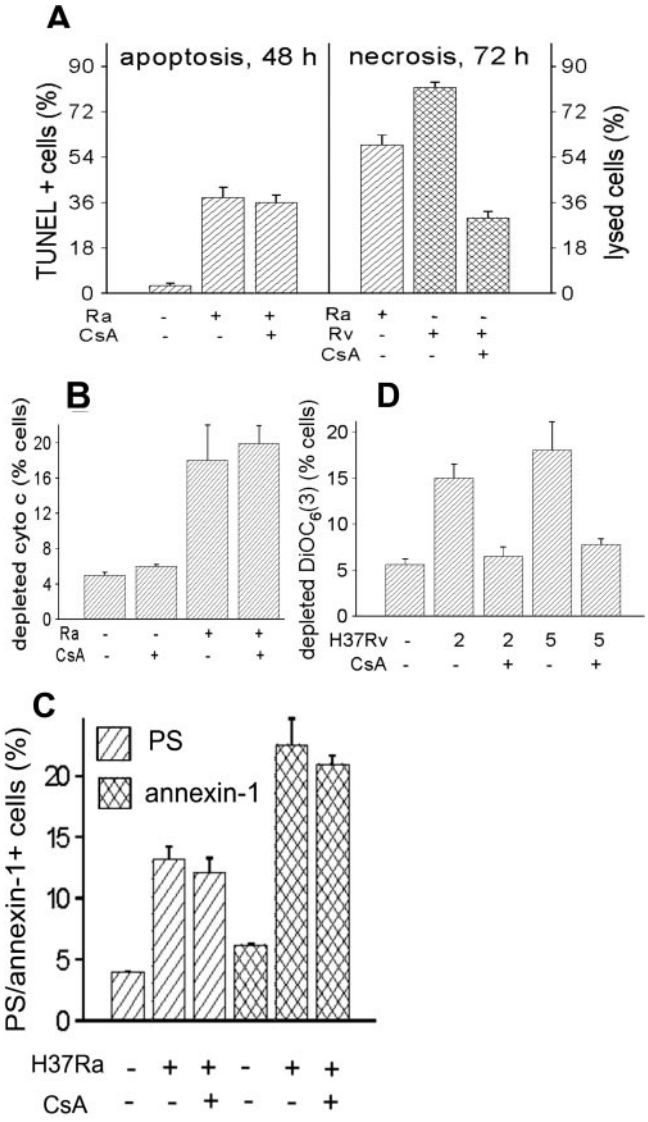

FIGURE 7. Induction of apoptosis measured by TUNEL cytochrome *c* release from the mitochondria, PS and annexin-1 exposure after infection of Mϕ with *Mtb* is not associated with MPT and loss of $\Delta\psi_m$. Mϕ infected in the presence and absence of the MPT inhibitor CsA (5 μM) with H37Ra or H37Rv (MOI 10 or the MOI indicated) were harvested at 48 or 72 h (*A*) or at 6 h (*B–D*). Shown are mean values ± SE for four experiments. *A*, Apoptosis of infected Mϕ measured by TUNEL assay (*left*) and necrosis of infected Mϕ measured by evaluation of cytolysis in the cultures using light microscopy (*right*). *B*, Cytochrome *c* release; *C*, PS and annexin-1 exposure. Apoptosis ($p < 0.20$), increase of the number of Mϕ with depleted cytochrome *c* ($p < 0.24$), and the increase of the number of Mϕ with augmented cell surface PS and annexin-1 ($p < 0.24$) are not blocked by CsA. In contrast, the increase in numbers of Mϕ with released cationic dye $DiOC_6(3)$ (*D*) and in numbers of necrotic Mϕ (*A*, *right*) is blocked by CsA. The number of Mϕ with depleted mitochondrial $DIOC_6(3)$ is significantly different for cells infected with H37Rv in the presence and absence of CsA ($p = 0.003$ for MOI 2; $p = 0.01$ for MOI 5), and necrosis is significantly inhibited by CsA ($p = 0.001$, $n = 3$).

specifically alter Ca^{2+} influx into the mitochondria, we show that both MPT and MOMP are dependent on mitochondrial calcium loading. As expected, inhibition of BAX activation blocks MOMP, but does not affect early transient $\Delta\psi_m$ dissipation. Moreover, the extent of transient $\Delta\psi_m$ dissipation in *Mtb*-infected Mϕ at 6 h correlates with the number of necrotic cells 48 h after infection. Cumulatively, these findings indicate that *Mtb* induce MOMP and

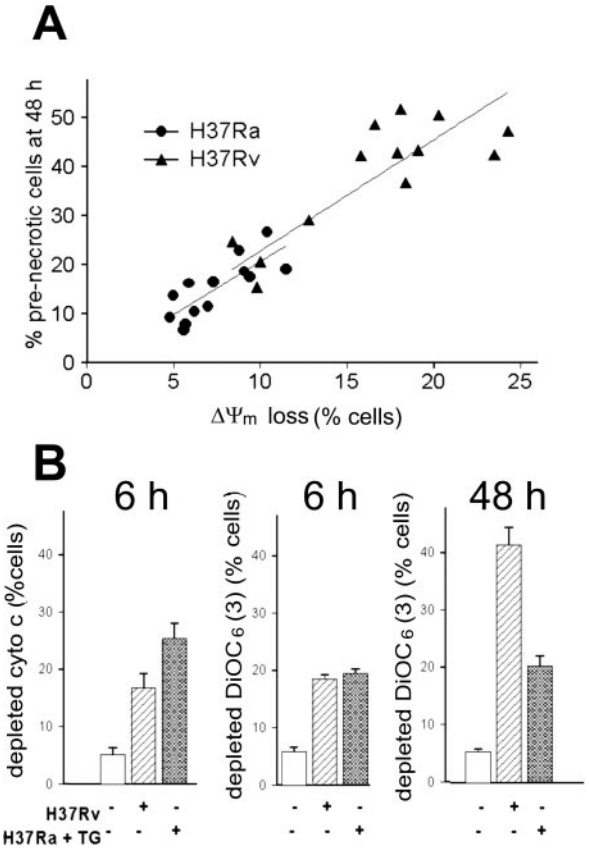

FIGURE 8. Correlation of $\Delta\psi_m$ loss and of cytochrome *c* release at 6 h with prenecrosis of *Mtb*-infected Mϕ at 48 h. *A*, Regression analysis comparing percentage of Mϕ undergoing $\Delta\psi_m$ loss at 6 h after infection with H37Ra (●) and H37Rv (▲) at various MOI vs percentage of prenecrotic Mϕ at 48 h ($p = 0.005$ and 0.007, for H37Ra and H37Rv, respectively). *B*, Increase of the numbers of Mϕ with increased MOMP at 6 h correlates with abrogation of prenecrosis at 48 h. Cells harvested at 6 h were analyzed for mitochondrial cytochrome *c* (MOMP, *left panel*) and $DiOC_6(3)$ ($\Delta\psi_m$ loss, *center panel*) release, and cells harvested at 48 h were analyzed for mitochondrial $DiOC_6(3)$ release as a marker of impending necrosis (*right panel*). Mϕ were infected with H37Ra (MOI 10) in presence of TG (0.1 μM) or with H37Rv (MOI 5) to obtain equal numbers of Mϕ with cationic dye release at 6 h (*center panel*). Shown are mean values ± SE for three experiments. Increased mitochondrial cytochrome *c* release at 6 h for H37Ra + TG relative to H37Rv ($p = 0.001$) correlates with decreased prenecrotic Mϕ at 48 h ($p = 0.001$). $\Delta\psi_m$ loss at 6 h is equalized ($p < 0.2$).

MPT by independent mechanisms, and that virulent *Mtb* induces significantly more MPT than attenuated bacilli.

MOMP causes the release from the mitochondria of caspase activators, including cytochrome *c*, that are normally sequestered between the inner and outer mitochondrial membrane (29) (see online supplement to Ref. 7). After release into the cytosol, cytochrome *c* forms a complex containing Apaf-1, ATP, and procaspase-9, resulting in the activation of downstream caspases (12) and apoptosis. Cytosolic cytochrome *c* also binds to inositol (1,4,5) triphosphate receptors of the endoplasmatic reticulum, amplifying the Ca^{2+} release from the endoplasmatic reticulum (30) that causes mitochondrial Ca^{2+} influx necessary for induction of apoptosis (31).

In contrast to apoptosis, necrosis is a consequence of the opening of the MPT pore (32). Components of this pore are adenine nucleotide translocase, the voltage-dependent anion transporter, and cyclophilin D, a small protein present inside the mitochondria that binds CsA and is involved in MPT (33). CsA prevents cyclophilin D binding to adenine nucleotide translocase, thereby inhibiting the opening of the MPT pore and MPT. In the case of infection with the virulent H37Rv when MPT is induced, irreversible mitochondrial damage ensues leading to necrosis and cytolysis of the affected cells. Thus, MPT is exploited by virulent *Mtb* to destroy the host cell, leading to spread of the infection.

An additional important mechanism that might be involved in the manifestation of apoptosis and might be suppressed by virulent *Mtb* is activation of plasma membrane repair mechanisms required for repair of damaged plasma membranes. These mechanisms require transiently increased intracellular Ca^{2+} concentration ($[Ca^{2+}]_i$) and use lysosomal membrane components to restore disrupted plasma membranes (34). Because necrosis is characterized by damage of the plasma membrane, we investigated whether increase of $[Ca^{2+}]_i$ required for the activation of plasma membrane repair mechanisms blocks necrosis. Addition of the ionophore A23187 to Mϕ, which increases $[Ca^{2+}]_i$, indeed down-regulates *Mtb*-induced necrosis (5), suggesting that Ca^{2+}-regulated repair mechanisms might be involved in maintaining the apoptotic state (35). This topic is currently under investigation in our laboratory.

There is a discrepancy between apoptosis and cytochrome *c* release, when the effects of avirulent and virulent *Mtb* strains are compared. Although apoptosis is more pronounced in H37Ra than in H37Rv-infected Mϕ cultures, cytochrome *c* release is similar in H37Rv and in H37Ra-infected Mϕ cultures. This paradox might by explained by the fact that in H37Rv-infected Mϕ cultures a significant number of the apoptotic cells has become necrotic, leading to a decrease of apoptotic Mϕ numbers in H37Rv-infected Mϕ cultures. In contrast, in H37Ra-infected Mϕ cultures, generation of necrotic cells is delayed and more apoptotic cells accumulate at any time point.

Several studies cite irreversible MPT as one of the key elements of caspase-dependent apoptosis (36, 37). Mitochondrial damage caused by MPT induces disruption of mitochondrial function by $\Delta\psi_m$ loss and consequent increase of reactive oxygen species production. Our findings differentiate between MTP and MOMP as effector mechanisms in *Mtb*-induced Mϕ death and corroborate findings of others that apoptosis is initiated in absence of mitochondrial permeability pore opening by MOMP (summarized in Ref. 7). MOMP is caspase and BAX dependent and does not affect the integrity of the mitochondria.

Furthermore, studies using mice with targeted disruption of cyclophilin D unable to undergo MPT and necrosis demonstrate that MOMP proceeds normally in these mice (38, 39). Cyclophilin D-deficient cells do not undergo CsA-sensitive mitochondrial membrane changes and are resistant to ischemia/reperfusion-induced necrosis, indicating that perturbation of the inner mitochondrial membrane regulates necrosis. Cyclophilin D deficiency does, however, not affect the release of cytochrome *c* from the mitochondria through MOMP, an event essential for the induction of apoptosis (39).

Recent findings suggest mechanisms that might partially explain the basis for MPT induction by virulent *Mtb* strains. Among the genes that are markedly down-regulated in the attenuated H37Ra in comparison with H37Rv are genes coding for members of the protein family containing 6-kDa early secretory Ag target (ESAT-6) (40), mycobacterial proteins that induce potent Th1 responses and elicit protection against tuberculosis (41) when administered as subunit or DNA vaccines (42). When bacillus Calmette-Guerin and *Mycobacterium bovis* were compared, the genes expressing ESAT-6 and culture filtrate protein-10 (*esxA* and *esxB*) were found to be part of the region of difference 1 (43). *esxA* and *esxB* are missing from the attenuated bacillus Calmette-Guerin, but are present in *M. bovis* and in virulent *Mtb* (44). ESAT-6 and culture-filtrated protein-10, which are secreted by the

bacilli as a tight 1:1 complex (45), can be pinocytosed by Mϕ and could act directly on the mitochondrial inner membrane, or, alternatively, might induce a factor(s) that disrupts the mitochondrial inner membrane.

Because the apoptotic state of the Mϕ has been linked to antimycobacterial activity (8) and enhanced Ag presentation (46), we propose that apoptosis of infected Mϕ is an innate defense mechanism that reduces the intracellular burden of *Mtb*, whereas necrosis promotes spread of the infection by cytolysis of the host Mϕ. Because <10 inhaled bacilli suffice to establish infection, our in vitro model with low MOI (<10) is particularly relevant to the early phase of *Mtb* exposure and development of human tuberculosis, indicating that the balance of apoptosis vs necrosis of infected Mϕ determines the course of *Mtb* infection in vivo. This concept is also supported by a recent study in the murine system (9), which shows that a host gene (*Ipr 1*) linked to tuberculosis resistance promotes apoptosis of infected Mϕ. Expression of the *Ipr1* transgene in *sst1*-susceptible Mϕ shifts the Mϕ death from necrosis to apoptosis. This process is associated with rescue of the infected Mϕ from MPT and an increase of PS on the cell surface.

An extraordinary, wide variety of conditions induces MPT, and at present there exists no consensus on a specific physiological role for this event (47). Our findings suggest that MPT plays a pivotal role in the evasion by virulent *Mtb* of the Mϕ's host defense. Induction of necrosis by virulent *Mtb* strains by triggering MPT allows release of the pathogens from the Mϕ, when the sanctuary of the host cell is no longer needed, while minimizing the antimicrobial effects of the Mϕ. Moreover, a functional connection between outer and inner mitochondrial membrane perturbation might exist, because release of factors from the mitochondrial intermembrane space due to MOMP might confer resistance to mitochondrial degradation and necrotic death, a consequence of MPT (Fig. 7*B*).

Thus, this study shows that *Mtb* are able to specifically alter the permeability of the mitochondrial outer and inner mitochondrial membranes of Mϕ, which determines whether the pathogens continue to remain sequestered within the host Mϕ or are released from the Mϕ by induction of necrosis, a distinctive capacity of virulent *Mtb* strains. Studies designed to understand the specific effects of the pathogens on the mitochondrial membranes and the role of mitochondrial factors either released from the mitochondrial intermembrane space or from the interior of the mitochondria in triggering programmed death will be of critical importance in the understanding of how *Mtb* modulates the innate immune system and how these systems can be altered to favor protection from progression from *Mtb* infection to tuberculosis.

Acknowledgments

We are grateful to Eileen Remold-O'Donnell for helpful discussions.

Disclosures

The authors have no financial conflict of interest.

References

1. Corbett, E. L., C. J. Watt, N. Walker, D. Maher, B. G. Williams, M. C. Raviglione, and C. Dye. 2003. The growing burden of tuberculosis: global trends and interactions with the HIV epidemic. *Arch. Intern. Med.* 163: 1009–1021.
2. Raviglione, M. C. 2003. The TB epidemic from 1992–2002. *Tuberculosis* 83: 4–14.
3. Leemans, J. C., N. P. Juffermans, S. Florquin, N. van Rooijen, M. J. Vervoordeldonk, A. Verbon, S. J. H. van Deventer, and T. van der Poll. 2001. Depletion of alveolar macrophages exerts protective effects in pulmonary tuberculosis in mice. *J. Immunol.* 166: 4604–4611.
4. Hingley-Wilson, S. M., L. M. Sly, N. E. Reiner, and W. R. McMaster. 2000. The immunobiology of the mycobacterial infected macrophage. *Mod. Aspects Immunobiol.* 1: 96–104.
5. Duan, L., H. Gan, D. E. Golan, and H. G. Remold. 2002. Critical role of mitochondrial damage in determining outcome of macrophage infection with *Mycobacterium tuberculosis*. *J. Immunol.* 169: 5181–5187.
6. Keane, J., H. G. Remold, and H. Kornfeld. 2000. Virulent *Mycobacterium tuberculosis* strains evade apoptosis of infected alveolar macrophages. *J. Immunol.* 164: 2016–2019.
7. Green, D. R., and G. Kroemer. 2004. The pathophysiology of mitochondrial cell death. *Science* 305: 626–629.
8. Fratazzi, C., R. D. Arbeit, C. Carini, and H. G. Remold. 1997. Programmed cell death of *Mycobacterium avium* serovar 4-infected human macrophages prevents the mycobacteria from spreading and induces mycobacterial growth inhibition by freshly added, uninfected macrophages. *J. Immunol.* 158: 4320–4327.
9. Pan, H., B.-S. Yan, M. Rojas, Y. V. Shebzukhov, H. Zhou, L. Kobzik, D. E. Higgins, M. J. Daly, B. R. Bloom, and I. Kramnik. 2005. *Ipr1* gene mediates innate immunity to tuberculosis. *Nature* 434: 767–772.
10. Green, D. R., and J. C. Reed. 1998. Mitochondria and apoptosis. *Science* 281: 1309–1312.
11. Li, P., D. Nijhawan, I. Budihardjo, S. M. Srinivasula, M. Ahmad, E. S. Alnemri, and X. Wang. 1997. Cytochrome *c* and dATP-dependent formation of Apaf-1/caspase-9 complex initiates an apoptotic protease cascade. *Cell* 91: 479–489.
12. Jiang, X., and X. Wang. 2000. Cytochrome *c* promotes caspase-9 activation by introducing nucleotide binding to Apaf-1. *J. Biol. Chem.* 275: 31119–31121.
13. Waterhouse, N. J., and J. A. Trapani. 2003. A new quantitative assay for cytochrome *c* release in apoptotic cells. *Cell Death Differ.* 10: 853–858.
14. Martin, S. J. C., P. M. Reutelingsperger, A. J. McGahon, J. A. Rader, R. C. A. A. van Schie, D. M. LaFace, and D. R. Green. 1995. Early redistribution of plasma membrane phosphatidylserine is a general feature of apoptosis regardless of the initiating stimulus: inhibition by overexpression of Bcl-2 and Abl. *J. Exp. Med.* 182: 1545–1556.
15. Arur, S., U. E. Uche, K. Rezaul, M. Fong, V. Scranton, A. E. Cowan, W. Mohler, and D. K. Han. 2003. Annexin 1 is an endogenous ligand that mediates apoptotic cell engulfment. *Dev. Cell* 4: 587–598.
16. Zamzami, N., P. Marchetti, M. Castedo, C. Zanin, J. L. Vayssiere, P. X. Petit, and G. Kroemer. 1995. Reduction in mitochondrial potential constitutes an early irreversible step of programmed lymphocyte death in vivo. *J. Exp. Med.* 181: 1661–1672.
17. Fadok, V. A., D. L. Bratton, and P. M. Henson. 2001. Phagocyte receptors for apoptotic cells: recognition, uptake and consequences. *J. Clin. Invest.* 108: 957–963.
18. Kroemer, G., B. Dallaporta, and M. Resche-Rigon. 1998. The mitochondrial death/life regulator in apoptosis and necrosis. *Annu. Rev. Physiol.* 60: 619–642.
19. Martinvalet, D., P. Zhu, and J. Lieberman. 2005. Granzyme A induces caspase-independent mitochondrial damage, a required first step for apoptosis. *Immunity* 22: 355–370.
20. Deshmukh, M., K. Kuida, and E. M. Johnson, Jr. 2000. Caspase inhibition extends the commitment to neuronal death beyond cytochrome *c* release to the point of mitochondrial depolarization. *J. Cell Biol.* 150: 131–143.
21. Szalai, G., R. Krishnamurthy, and G. Hajnoczky. 1999. Apoptosis driven by IP(3)-linked mitochondrial calcium signals. *EMBO J.* 18: 6349–6361.
22. Bernardi, P. 1999. Mitochondrial transport of cations: channels, exchangers and permeability transition. *Physiol. Rev.* 79: 1127–1155.
23. Broekemeier, K. M., R. J. Krebsbach, and D. R. Pfeiffer. 1994. Inhibition of the mitochondrial Ca^{++} uniporter by pure and impure ruthenium red. *Mol. Cell. Biochem.* 139: 33–40.
24. Thastrup, O., P. J. Cullen, B. K. Drøbak, M. R. Hanley, and A. P. Dawson. 1990. Thapsigargin, a tumor promoter, discharges intracellular Ca^{2+} stores by specific inhibition of the endoplasmic reticulum Ca^{2+}-ATPase. *Proc. Natl. Acad. Sci. USA* 87: 2466–2470.
25. Boitier, E., R. Rea, and M. R. Duchen. 1999. Mitochondria exert a negative feedback on the propagation of intracellular Ca^{2+} waves in rat cortical astrocytes. *J. Cell Biol.* 145: 795–808.
26. Keij, J. F., C. Bell-Prince, and J. A. Steinkamp. 2000. Staining of mitochondrial membranes with 10-nonyl acridine orange Mitofluor Green, and MitoTracker Green is affected by mitochondrial membrane potential altering drugs. *Cytometry* 39: 203–210.
27. Korsmeyer, S. J., M. C. Wei, M. Saito, S. Weiler, K. J. Oh, and P. H. Schlesinger. 2000. Pro-apoptotic cascade activates BID, which oligomerizes BAK or BAX into pores that result in the release of cytochrome *c*. *Cell Death Differ.* 7: 1166–1173.
28. Wei, M. C., W.-X. Zong, E. H.-Y. Cheng, T. Lindsten, V. Panoutsakopoulou, A. J. Ross, K. A. Roth, G. R. MacGregor, C. B. Thompson, and S. J. Korsmeyer. 2001. Proapoptotic BAX and BAK: a requisite gateway to mitochondrial dysfunction and death. *Science* 292: 727–730.
29. Li, P., D. Nijhawan, I. Budihardjo, S. M. Srinivasula, M. Ahmad, E. S. Alnemri, and X. Wang. 1997. Cytochrome *c* and dATP-dependent formation of Apaf-1/caspase 9 complex initiates apoptotic protease cascade. *Cell* 91: 479–488.
30. Boehning, D., R. L. Patterson, L. Sedaghat, N. O. Glebova, T. Kurosaki, and S. H. Snyder. 2003. Cytochrome *c* binds to inositol (1,4,5) triphosphate receptors, amplifying calcium-dependent apoptosis. *Nat. Cell Biol.* 5: 1051–1061.
31. Pinton, P., D. Ferrari, E. Rapizzi, F. Di Virgilio, T. Pozzan, and R. Rizzuto. 2001. The Ca^{2+} concentration of the endoplasmatic reticulum is a key determinant of ceramide-induced apoptosis: significance for the molecular mechanism of Bcl-2 action. *EMBO J.* 20: 2690–2701.
32. Halestrap, A. P., G. P. McStay, and S. J. Clarke. 2002. The permeability transition pore complex: another view. *Biochimie* 84: 153–166.
33. Halestrap, A. P., and A. M. Davidson. 1990. Inhibition of Ca^{2+}-induced large amplitude swelling of liver and heart mitochondria by cyclosporin A is probably

caused by the inhibitor binding to mitochondrial matrix peptidyl-prolyl *cis-trans* isomerase and preventing in interacting with the adenine nucleotide translocase. *Biochem. J.* 268: 153–160.
34. Reddy A., E. V. Caler, and N. W. Andrews. 2001. Plasma membrane repair is mediated by Ca^{2+}-regulated exocytosis of lysosomes. *Cell* 106: 157–169.
35. McNeil, P. L., and R. A. Steinhardt. 2003. Plasma membrane disruption: repair, prevention, adaptation. *Annu. Rev. Cell. Dev. Biol.* 19: 697–731.
36. Marchetti, P., M. Castedo, S. A. Susin, N. Zamzami, T. Hirsch, A. Macho, A. Haeffner, F. Hirsch, M. Geuskens, and G. Kroemer. 1996. Mitochondrial permeability transition is a central coordinating event of apoptosis. *J. Exp. Med.* 184: 1156–1160.
37. Li, H., H. Zhu, C. Xu, and J. Yuan. 1998. Cleavage of BID by caspase 8 mediates the mitochondrial damage in the Fas pathway of apoptosis. *Cell* 94: 491–501.
38. Baines, C. P., R. A. Kaiser, N. H. Purcell, N. S. Blair, H. Osinska, M. A. Hambleton, E. W. Brunskill, M. R. Sayen, R. A. Gottlieb, G. W. Dorn, et al. 2005. Loss of cyclophilin D reveals a critical role for mitochondrial permeability transition in cell death. *Nature* 434: 658–662.
39. Nakagawa, T., S. Shimizu, T. Watanabe, O. Yamaguchi, K. Otsu, H. Yamagata, H. Inohara, T. Kubo, and Y. Tsujimoto. 2005. Cyclophilin D-dependent mitochondrial permeability transition regulates some necrotic but not apoptotic cell death. *Nature* 434: 652–658.
40. Rindi, L., N. Lari, and C. Gazelli. 1999. Search for genes potentially involved in *Mycobacterium tuberculosis* virulence by mRNA differential display. *Biochem. Biophys. Res. Commun.* 258: 94–101.
41. Brandt, L., T. Oettinger, A. Holm, and P. Andersen. 1996. Key epitopes on the ESAT-6 antigen recognized in mice during the recall of protective immunity to *Mycobacterium tuberculosis*. *J. Immunol.* 157: 3527–3533.
42. Brandt, L., M. Elhay, I. Rosenkrands, E. B. Lindblad, and P. Andersen. ESAT-6 subunit vaccination against *Mycobacterium tuberculosis*. 2000. *Infect. Immun.* 68: 791–795.
43. Mahairas, G. G., P. J. Sabo, M. J. Hickey, D. C. Singh, and C. K. Stover. 1996. Molecular analysis of genetic differences between *Mycobacterium bovis* BCG and virulent *M. bovis*. *J. Bacteriol.* 178: 1274–1282.
44. Behr, M. A., M. A. Wilson, W. P. Gill, H. Salamon, G. K. Schoolink, S. Rane, and P. M. Small. 1999. Comparative genomics of BCG vaccines by whole-genome DNA microarray. *Science* 284: 1520–1523.
45. Renshaw, P. S., P. Panagiotidou, A. Whelan, S. V. Gordon, R. G. Hewinson, R. A. Williamson, and M. D. Carr. 2002. Conclusive evidence that the major T-cell antigens of the *Mycobacterium tuberculosis* complex ESAT-6 and CFP-10 form a tight, 1:1 complex and characterization of the structural properties of ESAT-6, CFP-10, and the ESAT-6-CFP-10 complex. *J. Biol. Chem.* 277: 21598–21603.
46. Schaible, U. E., F. Winau, P. A. Sieling, K. Fischer, H. L. Collins, K. Hagens, R. L. Modlin, V. Brinkmann, and S. H. E. Kaufmann. 2003. Apoptosis facilitates antigen presentation to T lymphocytes through MHC-I and CD1 in tuberculosis. *Nat. Med.* 9: 1039–1046.
47. Zoratti, M., and I. Szabó. 1995. The mitochondrial permeability transition. *Biochim. Biophys. Acta* 1241: 139–176.